GRAIN SIZE CONTROL IN RING-ROLLED ALLOY 718

D.R. Nielsen*, S.W. Thompson, C.J. Van Tyne and M.C. Mataya**

Advanced Steel Processing and Products Research Center
Colorado School of Mines
Golden, CO 80401
U.S.A.

Abstract

The controllable independent variables for the processing of ring-rolled alloy 718 were investigated to determine which were influential in affecting the final microstructure. A Taguchi technique for experimental design was employed to determine the critical independent variables. The variables investigated included: deformation temperature, hold time at temperature prior to deformation, cooling during deformation, cooling after deformation, number of deformation passes, total reduction, strain rate, and initial grain size. From an analysis of variance (ANOVA), the influence of each independent variable on the final microstructure and properties was determined. The measured response variables were percent recrystallization, recrystallized grain size, room-temperature hardness, and high-temperature flow stress. Results of the study revealed that deformation temperature and total reduction were the critical variables in determining percent recrystallization. Recrystallized grain size was dependent on deformation temperature and cooling during deformation, which together determine the finishing temperature. Cooling rate after deformation was the dominant variable affecting hardness. Temperature and strain rate were the critical variables affecting flow stress.

* Now with Chrysler Corporation, Auburn Hills, MI, USA.
** EG & G Rocky Flats, Golden, CO, USA.

Superalloys 718, 625, 706 and Various Derivatives
Edited by E.A. Loria
The Minerals, Metals & Materials Society, 1994

Introduction

Background on Alloy 718

Alloy 718 is a nickel-base superalloy that exhibits high strength and ductility, and high fatigue and corrosion resistance for extended times at temperatures up to 650°C (1200°F). This temperature is a 150°C (300°F) improvement over stainless steels and titanium alloys. These favorable properties at a relatively inexpensive price have made alloy 718 the most dominant superalloy in production, consisting of approximately 45% of the total tonnage of nickel-based alloys in wrought form and 25% in cast form (1). Extensive use of 718 is found in the aerospace, petrochemical, and nuclear industries (2).

The strengthening and heat-resistant properties of alloy 718 are due mainly to the precipitation of two phases, gamma prime (γ') and gamma double prime (γ''), upon aging. Gamma prime is a coherent ordered $Ni_3(Al,Ti,Nb)$ fcc $L1_2$ structure. This phase is a strengthening component in most Ni- and Ni-Fe-based alloys. Gamma double prime is a coherent Ni_3Nb bct DO_{22} structure. In nickel alloys of high niobium content, such as alloy 718, this phase becomes the primary strengthening precipitate. The strengthening imparted by precipitation of γ' and γ'' is due mainly to coherency strains between the matrix and the precipitates, with some strengthening due to the occurrence of antiphase domain boundaries (3). The degradation of mechanical properties at extended times above 650°C (1200°F) is a result of the formation of the brittle delta (δ) phase in favor of γ''. The δ phase is the equilibrium phase of the metastable γ'' and has the same Ni_3Nb stoichiometry as γ''; however, δ has an orthorhombic DO_a structure that is incoherent with the matrix. At temperatures below 650°C, γ'' nucleates in favor of δ because the much lower interfacial and strain energy components of γ'' more than compensate for the higher chemical driving force associated with the equilibrium δ phase (4,5). Above 650°C, δ may precipitate preferentially to γ'' or the γ'' to δ transformation may occur, resulting in loss of coherency strain and strength. The kinetics of this transformation, dependent on temperature and degree of supersaturation of the hardening components, establishes the time/temperature limits of alloy 718 in jet-engine applications.

A fine-grained alloy 718 product is often desirable. It is well recognized that fine-grained structures exhibit higher tensile properties and toughness, as well as improved high-cycle fatigue performance and cycles to crack initiation (6,7). For example, Brown, Boettner, and Ruckle found that when grain size was reduced from ASTM 3 to ASTM 12, fatigue strength doubled (7). A uniform fine-grained microstructure can be developed by manipulation of the thermomechanical processing (TMP) of the alloy 718 workpiece. The level of microstructural refinement by TMP is strongly related to three major factors 1) the reheating behavior, 2) the hot-deformation schedule and 3) the transformation behavior (8). During reheating, events may occur, depending on the starting microstructure, that will influence the hot deformation and resultant transformations. These events include nucleation, growth and possible grain coarsening, reduction in inhomogeneities of solute distribution, and dissolution of precipitates. The hot-deformation schedule, the amount and rate of work on the material at temperature, and the transformation behavior of the metal determines the as-deformed microstructure: fully recrystallized, partially recrystallized, or fully unrecrystallized. By employing the proper hot-deformation processes, a fine-grained fully recrystallized structure can be obtained.

Ring Rolling

Ring rolling is a metal forming process for manufacturing seamless ring forgings. It involves piercing a hole in a heated cylindrical blank, thereby producing a doughnut-shaped workpiece for rolling. When the workpiece is placed on the ring-rolling mill, the hole fits over a mandrel, which is slightly smaller in diameter than the inner diameter of the ring. The wall of the blank is positioned between the mandrel and the larger diameter main roll as shown in Figure 1. The main roll rotates and is pressed into the workpiece. The friction between the roll and the ring causes rotation of the ring, which in turn, causes rotation of the mandrel. The roll gap between the mandrel and the main roll is progressively reduced either through automated or manual control, reducing the ring thickness. The ring diameter grows due to circumferential extension in the direction of the ring rotation as a result of reduction in the radial cross section. The height of the ring may be controlled by upset forging the ring between passes or through the implementation of radial axial rolls set diametrically across the ring from the main roll and mandrel as shown in Figure 1.

Depending on the size of the ring, cooling may occur during forming due to radiation and convection losses that are not offset by deformation heating. As the loss in heat results in greatly increased rolling force, the

ing may be removed, reheated, and placed back in the mill for continued reduction. Each uninterrupted deformation cycle is termed a "pass."

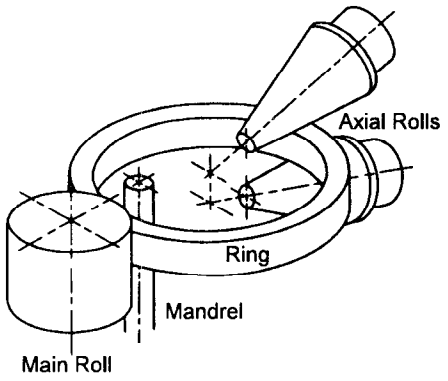

Figure 1 - Schematic of radial-axial mill. Axial rolls maintain height of ring, main roll and mandrel reduce ring thickness.

Objective of Study

The primary goal of this study is to determine the processing conditions necessary to produce a fine grain size in ring-rolled alloy 718. The industrial processing conditions examined and simulated in the laboratory experiments spanned the initial heating of the ring, through the various reduction passes in the rolls, to the cooling procedure following the final pass. This study also determines the critical independent variables for ring rolling.

In an alloy 718 ring produced via ring rolling, the thermomechanical processing the ring receives during fabrication defines the microstructure, and therefore the properties of the ring, prior to heat treatment for precipitation strengthening. Ideally, a thermomechanical processing scheme will exploit temperature, strain rate and strain interactions to produce a desired microstructure to enhance the properties of the workpiece (9). For example, deformation at relatively low hot-working temperatures, high strain rates, and to high strains produces a fine-grained microstructure which is associated with increased tensile strength and fatigue properties. However, deformation at low hot-working temperatures must be weighed against the possible precipitation of detrimental phases, such as δ, during deformation.

The method used in this study to determine which of the controllable variables in the process critically affect final microstructure was an experimental test plan based on an orthogonal test matrix utilizing Taguchi techniques for experimental design. Application of Taguchi techniques for experimental design along with analysis of variance (ANOVA) was used to determine the statistically influential independent variables (10).

This paper will deal exclusively with the effects of the finishing passes which are typically applied to alloy 718 during ring rolling. Information pertaining to melting, casting, homogenization, and hot working of as-cast alloy 718 has been presented in other papers (11-16).

Experimental Procedures

Characterization of As-Received Material

Specimens for hot-deformation testing were obtained as 114 mm (4.5 in) long by 15 mm (0.60 in) diameter bars. The specimens were obtained from a previously processed ring. Figure 2 is a schematic diagram which shows the location of the sample bars relative to the rolled ring. The chemical composition of the bars is given in Table I.

Table I - Chemical Composition of Alloy 718 Used in Experimentation

Element	Ni	Fe	Cr	Nb	Mo	Ti	Al	Co
(wt%)	52.58	18.97	18.34	5.16	3.02	1.00	0.57	0.26
Element	Si	Mn	Cu	C	P	B	S	
(wt%)	0.11	0.10	0.058	0.037	0.007	0.004	< 0.001	

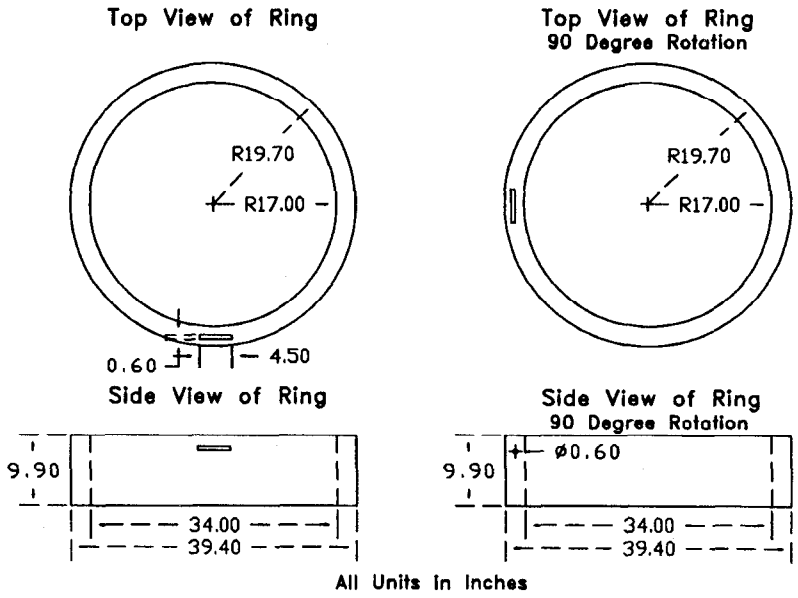

Figure 2 - Schematic of sample bars taken from as-forged ring.

Figure 3 shows light micrographs of the as-received material. Figure 3a shows the microstructure parallel to the rolling direction. There exists a large variation of both grain size and shape. Many of the grains are elongated and little recrystallization is evident. A high concentration of deformed annealing twins is present. Deformed annealing twins are identified by the curvature associated with the twin boundary. Both elongated grains and the deformed twins indicate the presence of a high dislocation density (*i.e.*, cold work) in this structure. Particles are distributed sparsely at the grain boundaries and throughout the matrix. Figure 3b shows the microstructure transverse to the rolling direction. The grains in this section appear to have somewhat greater directionality and elongation than those observed in the other section. Deformed annealing twins are also present.

Figures 4a and 4b show scanning electron micrographs of the transverse section of as-received material. Both blocky and needlelike particles are observed predominantly at the grain boundaries and sparsely distributed within the grain. These particles appear to be arranged in four orientation variants. It is believed that these precipitates are the δ phase. An energy dispersive spectroscopy (EDS) spectrum was obtained from a single needle precipitate, but the size of the particle was too small to allow definitive identification via this technique.

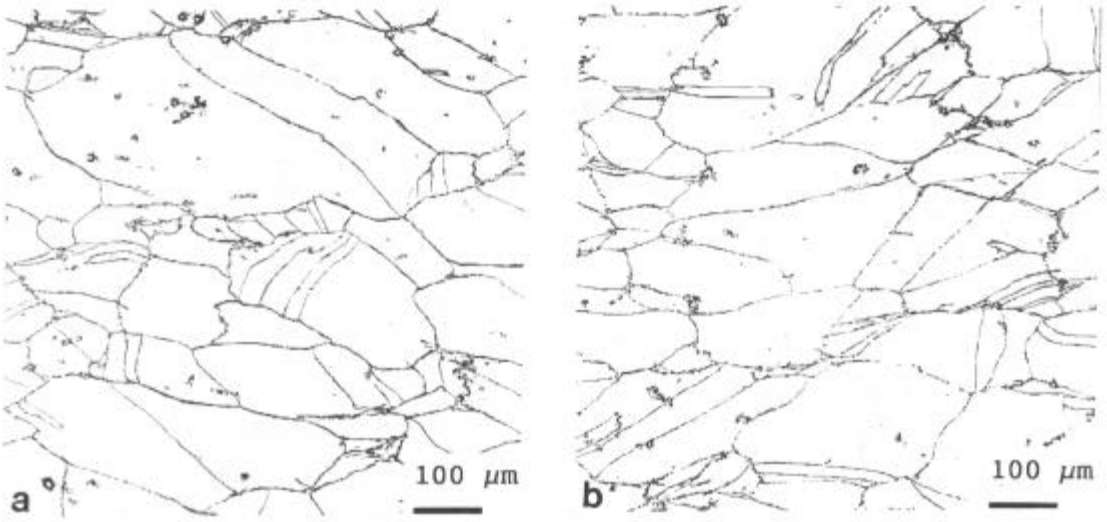

Figure 3 - Light micrographs of initial material from an as-forged ring. a) Parallel to rolling direction. b) Transverse to rolling direction. Electrolytic etch using 10% oxalic acid.

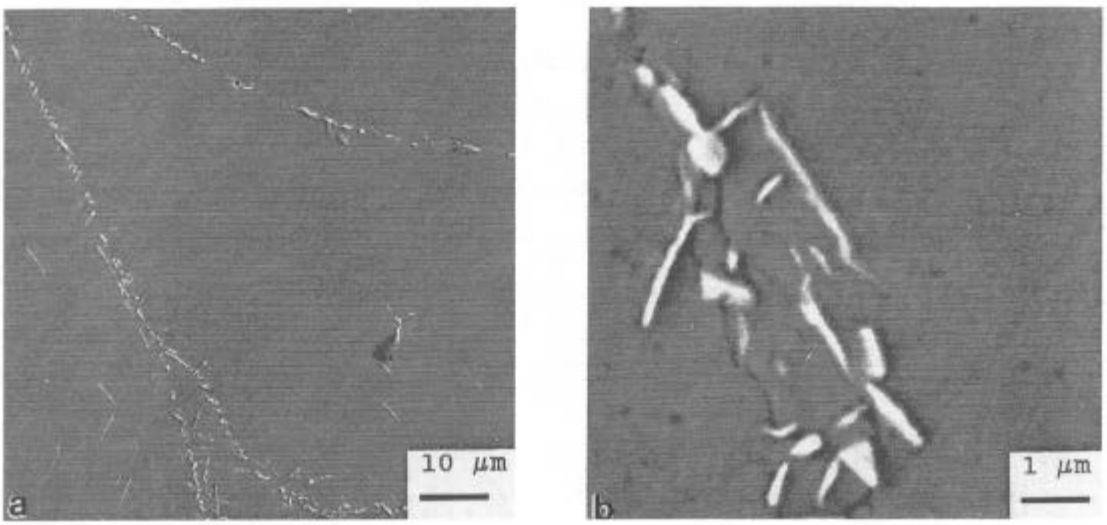

Figure 4 - SEM micrographs of transverse section showing needlelike δ-phase and blocky carbonitrides. a) Low magnification. b) High magnification

Figure 4b shows several micron-sized blocky precipitates along a grain boundary. These blocky precipitates were also seen sporadically within the grains. The EDS spectrum from a blocky particle indicated that it is niobium rich with a small amount of titanium. It is believed that these precipitates are (Nb,Ti)(C,N) (*i.e.*, niobium/titanium carbonitrides).

Description of Taguchi Techniques for Experimental Design

Due to the large number of independent variables in the ring-rolling process, a full-factorial test matrix is an unrealistic approach since the time and material available are not sufficient. Therefore the Taguchi method for experimental design has been incorporated to formulate a condensed, yet viable, testing procedure.

The Taguchi method allows the evaluation of several independent variables (factors) with a minimum number of tests. Taguchi's method of experimental design utilizes orthogonal arrays in place of a full compliment of testing of all the independent variables. Orthogonal arrays were developed from test plans referred to as fractional factorial experimentation (FFE) (10). FFE uses only a portion of the total possible combinations of factors and parameter levels to estimate the effect of the main factors and pertinent interactions of the main factors on response variables in the final product. An example of the condensing power obtained by the Taguchi method in determining the influential factors in an experiment is as follows. If there are eight factors (*i.e.*, independent variables) at two levels each (*e.g.*, a high value and a low value), a full-factorial experiment would require 2^8 or 256 individual trials and subsequent analysis of each trial. For this type of experiment with the Taguchi method, an L16 orthogonal test matrix would be used, requiring only 16 tests (10).

The interpretation of the experimental data received, via tests run employing an orthogonal test matrix, is made using a statistical method known as analysis of variance (ANOVA). This type of analysis can determine, in a statistical sense, the critical factor or factors for controlling the variation in the product response. It is important to note that this Taguchi method provides nothing more than a statistical evaluation of the data. It does not give insight into the mechanism(s) or phenomenological processes that are taking place within the material. To provide useful metallurgical information with respect to why a particular factor has the statistical significance that it does, further experimental analysis needs to be performed.

Table II - Independent Variables and Levels for Taguchi Tests

Column in Orthogonal Test Matrix	Independent Variable	Variable Symbol	Level 1 (Low)	Level 2 (High)	Units
1	Starting temperature	T_o	1010	1120	°C
2	Initial hold time	t_o	1.5	15	min
3	Interaction of T_o and t_o				
4	Cooling during deformation	ΔT_D	0	55.5	°C
5	Interaction of T_o and ΔT_D				
7	Cooling rate after deformation	$\dot{C}$	33.3	167	°C/min
8	Number of rolling passes*	N	1	3	
11	Total gage reduction	r	35	70	%
13	Strain rate	$\dot{\epsilon}$	0.1	0.95	s^{-1}
14	Starting grain size	D_o	1	4.4	ASTM

* Five hits per pass

Application of Taguchi Method to Ring-Rolling Simulation

Table II lists the independent variables under consideration for the simulation of the ring-rolling process. Also listed are the two levels of each variable. The independent variables and their parameters were determined through discussions with industrial ring rollers and by experimental limitations of the laboratory facilities.

Two levels of each factor are used to minimize the number of trials. The factor levels were initially chosen to approximate as closely as possible the range that the given variable may encounter in industrial processing. Starting temperature levels were chosen to provide the range attempted in large-scale rolling. Initial hold time characterizes the time that a ring heated to temperature may be held in the furnace prior to deformation. Hold times in actual processing of rings may be much longer due to scheduling problems that may arise in production; however, it was felt that a 15 minute hold time was long enough to produce any significant difference in results in the response variables if initial hold time was to be a statistically significant variable. The interaction of starting temperature and hold time was also considered to a possibly important factor; hence it was chosen as a variable for examination in the Taguchi orthogonal array.

Cooling during deformation can occur depending on the size, temperature, and rotational speed of the ring during rolling due to convection, radiation, and conduction losses. Adiabatic heating can offset this process. The factor levels for this variable were determined from optical pyrometer readings of the surface of a number of rings which were processed by industry. The interaction of starting temperature and cooling during deformation was also considered.

The high and low levels for cooling rate after deformation were chosen to give a spread between the levels to allow the Taguchi setup to estimate any statistical significance of cooling rate to any response variables. The number of rolling passes pertains to the number of times the ring is deformed via ring rolling, removed from the rolls, reheated, and placed back between the rolls for further reduction.

Between each pass, a 1.5-minute hold time is given at the temperature, or the piece is reheated to the deformation temperature if cooling during deformation is scheduled for a given test. This simulates the ring being placed in a furnace for reheat between passes. A 1.5-minute hold time was chosen for time conservation.

Total reduction was chosen based on industrial processing. For more than one pass, the reduction was divided evenly among the passes with respect to true strain. Strain rate levels were estimated from calculations of the amount of reduction occurring to a section of the ring in contact with the rolls at a given time, divided by the time that section of the ring will pass through the rolls. The range of starting grain sizes was chosen through discussions with industry. Table II also lists the column number that corresponds to each variable in the orthogonal test matrix.

The 16 hot-deformation trials were run with the parameters set as described above. Upon completion of each trial the specimen underwent the following analyses:

1. Measurement of percent recrystallization.
2. Measurement of recrystallized grain size.
3. Hardness testing.
4. Load at 3.0-mm stroke displacement, which corresponds directly to the flow stress at this strain.

These analyses are the quantifiable response variables for this set of tests. Each of the response variables is analyzed via ANOVA to determine which factor or factors have the largest statistical influence on it.

Specimen Preparation for Hot-Deformation Testing

Seven of the eight independent variables are directly controlled through the programming of the Colorado School of Mines Gleeble 1500 thermal-mechanical testing system, on which the hot deformation testing was performed. The remaining variable, starting grain size, was produced prior to testing. Appropriate heat treatments to obtain the desired initial grain sizes for hot deformation testing were determined. One bar of as-received material was sectioned into ten 6.4-mm (0.25-in.) disks. Five disks were heat treated at 1000°C to 1100°C (1832°F- 2012°F) at 25°C intervals for one hour to determine the conditions to reproduce an

ASTM grain size 1. An ASTM 1 grain size (229 μm diameter) was obtained from a one-hour solutionizing at 1100°C (2012°F). Two of the as-received bars received this heat treatment. Five more disks were heat treated at 1000°C (1832°F), varying the time from 10 to 50 minutes to determine the conditions for producing as fine a recrystallized grain size as possible from the as-received material. Unsatisfactory results from these heat treatments led to further testing. Twenty minutes solutionizing at 1025°C (1877°F), producing an ASTM 4.4 (72 μm), was found to be the optimum treatment. Two additional as-received bars were given this heat treatment. Upon completion of heat treating, the bars were machined to a diameter of 10 mm (0.39 in.) and cut into 12-mm (0.47-in.) long cylinders for testing.

Micrographs of the fine- and coarse-grained starting microstructure for the Taguchi experiment are shown in Figures 5a and 5b. Close examination of the fine-grained structure reveals some "ghost" boundaries, *i.e.*, linear arrays of particles which reside on prior grain boundaries. These ghost boundaries have been observed in many of the specimens that were heat treated in the attempt to obtain a fine-grain size. The precipitates were completely dissolved in the specimens heat treated at higher temperatures which produced the coarse-grain size specimens and no "ghost" boundaries were observed.

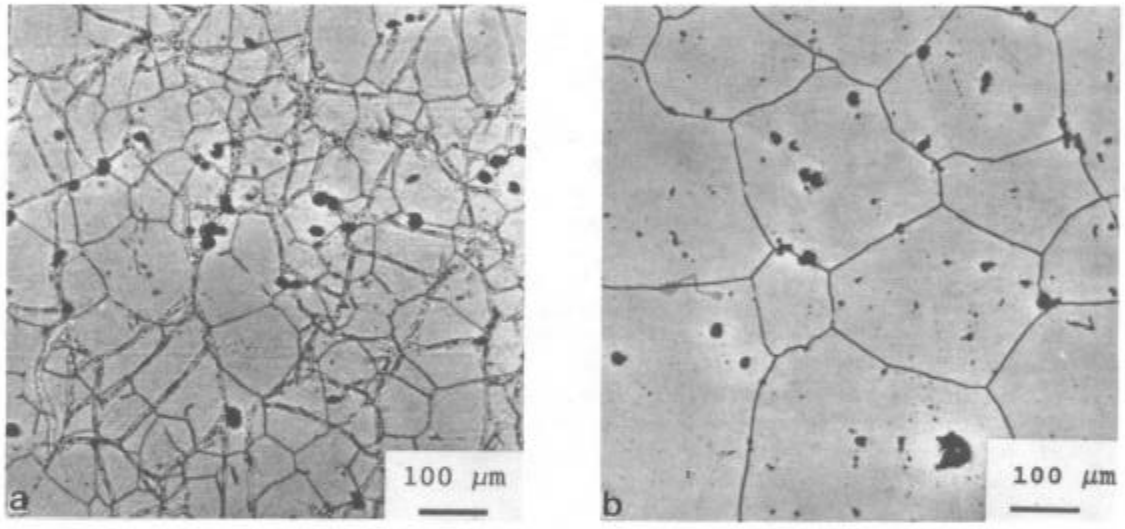

Figure 5. a) Light micrograph of fine-grained starting microstructure for hot-deformation testing. b) Light micrograph of coarse-grained starting microstructure for hot-deformation testing.

Hot-Deformation Testing

All hot-deformation testing of alloy 718 specimens was performed on the Gleeble 1500 dynamic thermal-mechanical testing machine. With the Gleeble 1500, one is able to simulate closely, under precise control, the thermal-mechanical conditions of large-scale ring rolling as well as other forging processes. The Gleeble 1500 uses a closed loop servo-hydraulic system that controls the mechanical variables and a resistance heating system that provides rapid heating and cooling rates with fairly uniform temperature profiles throughout the cross sections of the specimen. The test parameters for each of the sixteen tests are shown in Table III.

Table III - Independent Parameter Values for Each Taguchi Test

Test	T-1	Test	T-2	Test	T-3	Test	T-4
T_o	1010°C	T_o	1010°C	T_o	1010°C	T_o	1010°C
t_o	1.5 min	t_o	1.5 min	t_o	1.5 min	t_o	1.5 min
ΔT_D	0	ΔT_D	0	ΔT_D	55.5°C	ΔT_D	55.5°C
$\dot{C}$	33.3°C/min	$\dot{C}$	33.3°C/min	$\dot{C}$	167°C/min	$\dot{C}$	167°C/min
N	1	N	3	N	1	N	3
r	35%	r	70%	r	35%	r	70%
$\dot{\epsilon}$	$0.1s^{-1}$	$\dot{\epsilon}$	$0.95s^{-1}$	$\dot{\epsilon}$	$0.95s^{-1}$	$\dot{\epsilon}$	$0.1s^{-1}$
D_o	ASTM 1	D_o	ASTM 4.4	D_o	ASTM 4.4	D_o	ASTM 1

Test	T-5	Test	T-6	Test	T-7	Test	T-8
T_o	1010°C	T_o	1010°C	T_o	1010°C	T_o	1010°C
t_o	15 min	t_o	15 min	t_o	15 min	t_o	15 min
ΔT_D	0	ΔT_D	0	ΔT_D	55.5°C	ΔT_D	55.5°C
$\dot{C}$	167°C/min	$\dot{C}$	167°C/min	$\dot{C}$	33.3°C/min	$\dot{C}$	33.3°C/min
N	1	N	3	N	1	N	3
r	70%	r	35%	r	70%	r	35%
$\dot{\epsilon}$	$0.1s^{-1}$	$\dot{\epsilon}$	$0.95s^{-1}$	$\dot{\epsilon}$	$0.95s^{-1}$	$\dot{\epsilon}$	$0.1s^{-1}$
D_o	ASTM 4.4	D_o	ASTM 1	D_o	ASTM 1	D_o	ASTM 4.4

Test	T-9	Test	T-10	Test	T-11	Test	T-12
T_o	1120°C	T_o	1120°C	T_o	1120°C	T_o	1120°C
t_o	1.5 min	t_o	1.5 min	t_o	1.5 min	t_o	1.5 min
ΔT_D	0	ΔT_D	0	ΔT_D	55.5°C	ΔT_D	55.5°C
$\dot{C}$	167°C/min	$\dot{C}$	167°C/min	$\dot{C}$	33.3°C/min	$\dot{C}$	33.3°C/min
N	1	N	3	N	1	N	3
r	70%	r	35%	r	70%	r	35%
$\dot{\epsilon}$	$0.95s^{-1}$	$\dot{\epsilon}$	$0.1s^{-1}$	$\dot{\epsilon}$	$0.1s^{-1}$	$\dot{\epsilon}$	$0.95s^{-1}$
D_o	ASTM 1	D_o	ASTM 4.4	D_o	ASTM 4.4	D_o	ASTM 1

Test	T-13	Test	T-14	Test	T-15	Test	T-16
T_o	1120°C	T_o	1120°C	T_o	1120°C	T_o	1120°C
t_o	15 min	t_o	15 min	t_o	15 min	t_o	15 min
ΔT_D	0	ΔT_D	0	ΔT_D	55.5°C	ΔT_D	55.5°C
$\dot{C}$	33.3°C/min	$\dot{C}$	33.3°C/min	$\dot{C}$	167°C/min	$\dot{C}$	167°C/min
N	1	N	3	N	1	N	3
r	35%	r	70%	r	35%	r	70%
$\dot{\epsilon}$	$0.95s^{-1}$	$\dot{\epsilon}$	$0.1s^{-1}$	$\dot{\epsilon}$	$0.1s^{-1}$	$\dot{\epsilon}$	$0.95s^{-1}$
D_o	ASTM 4.4	D_o	ASTM 1	D_o	ASTM 1	D_o	ASTM 4.4

T_o	Deformation temperature	N	Number of passes
t_o	Hold time	r	Percent reduction
ΔT_D	Cooling during deformation	$\dot{\epsilon}$	Strain rate
$\dot{C}$	Cooling rate after deformation	D_o	Grain size

Assessment of Response Variables

Upon completion of the hot-deformation Gleeble tests, specimens were sectioned into longitudinal and transverse pieces, mounted, polished and etched. Micrographs were taken of the longitudinal and transverse sections of each of the sixteen Taguchi test specimens. Test numbers are designated as T-1 for test number one, through T-16 for Taguchi test sixteen. Values for percent recrystallization were obtained by point counting with a 100-point grid. Magnification was determined by the lowest magnification capable of discerning recrystallized from unrecrystallized areas. Recrystallization grain size was determined via standard linear intercept methods. Hardness was measured on a digital Rockwell hardness tester. Load at 3.0 mm stroke displacement was obtained from load-versus-displacement curve obtained during the test. Each of the response variables was analyzed via ANOVA to determine which of the independent variable(s) had the largest statistical influence on the given response variable.

Taguchi Test Results and Discussion

The measured values for the response variables are given in Table IV.

Table IV - Response Variables for ANOVA

Test No.	Recrystallization (%)		Recrystallized Grain Size (μm)	Hardness (HRC)		Load at 3.0 mm Displacement (kg_f)
	Long.	Trans.	(Long. + Trans.)/2	Long.	Trans.	
T-1	42	38	15	29	30	2280
T-2	100	100	25	31	30	2820
T-3	19	18	4	25	24	3040
T-4	69	61	10	26	26	2660
T-5	87	74	8	24	24	2040
T-6	70	76	16	18	20	2160
T-7	80	72	8	32	24	3580
T-8	6	5	6	34	32	2450
T-9	100	100	75	12	14	1790
T-10	100	100	58	13	13	1200
T-11	100	100	30	31	19*	1300
T-12	100	100	46	26	29	1490
T-13	100	100	74	29	30	1720
T-14	100	100	113	29	32	1210
T-15	64	64	22	15	16	1500
T-16	100	100	22	17	18	2120

* very thin specimen

Long. = Longitudinal
Trans. = Transverse

Specimens Deformed at 1010°C

Tests T-1 through T-8 were performed at the lower working temperature of 1010°C (1850°F). All specimens deformeded at 1010°C exhibited a duplex grain size microstructure, with the exception of test T-2, which was completely recrystallized. Figure 6 shows examples of the varying types of microstructures observed. Recrystallization had occurred to some extent in all specimens, ranging from the appearance of fine nuclei on the grain boundaries for T-1 to complete recrystallization for test T-2. Recrystallization occurred at preexisting grain boundaries, annealing twins, and carbonitrides, resulting in either a necklace-type microstructure in some specimens or near complete recrystallization with sporadic unrecrystallized areas.

The micrograph shown in Figure 6a is from test T-1 revealing the necklace type microstructure from the nucleation of grains on prior annealing twin boundaries and grain boundaries. Test T-1 achieved approximately 40% recrystallization with a recrystallized grain size of 15 μm. Results of the ANOVA procedure showed that temperature and percent reduction (*i.e.*, strain) were the statistically influential factors in determining the amount of recrystallization.

The microstructure of test T-2 is shown in Figure 6b. The fine-grain size and absence of deformed annealing twins indicates that 100% recrystallization has taken place. The grains do not exhibit an ideal, uniform, equiaxed structure, as seen at the high-temperature tests, and a number of small annealing twins are present, also not observed in the high-temperature tests. It has been mentioned previously that recrystallization of alloy 718 may occur through twinning. A study of a nickel-based alloy was performed to determine the role of twin boundaries in recrystallization and grain growth (17). It found that recrystallization occurs under conditions at which, not withstanding very high temperatures, the normal migration of grain boundaries is impeded because of a barrier effect from a large dispersion of insoluble particles. Under these conditions the boundary energy can be decreased by splitting it into a coherent and incoherent boundary, with the coherent boundary assuming a stepwise shape. This process becomes more energetically favorable in materials with low twin boundary energies, and therefore low stacking-fault energies. Further, it was found that immediately after hot deformation twin boundaries were found in every sixth grain. Upon annealing to 1210°C for 2.5 hours, twins appeared in every third grain, and after continued annealing, in every second grain. However on completion of the coarsening and formation of large uniform grains, twin boundaries began to disappear to again lower the internal energy of the grains. This study indicates that at a low forging temperature, recrystallization by twinning may be energetically favorable due to fine precipitates creating a boundary for large-angle motion. Twins were observed in all the low-temperature tests. In low-temperature tests in which cooling during deformation occurs, it would be plausible that δ precipitates may form a barrier resulting in twinning. However, at 1010°C, all δ should be dissolved and annealing twins would have to be caused by some other barrier, fine carbonitrides or solute drag. No twins are present in the higher-temperature tests indicating either that recrystallization did not occur via twinning, and therefore the barrier was removed at higher temperatures, or the twin boundaries disappeared upon structure coarsening. Referring back to test T-2, the factors giving a 100% recrystallized structure are: 1) 70% reduction which increases the density of the dislocation substructure and also increases the driving force and kinetics for the strain relieving mechanisms such as recrystallization and/or recovery; 2) Absence of cooling during deformation so that the specimen remains above the δ-solvus temperature, where δ is known to retard recrystallization (16). If cooling occurred, the 55.5°C (100°F) temperature decrease would have been detrimental to recrystallization which is a time-temperature-dependent process (18). Test T-2 was given passes which leads to an extra three minutes at temperature as compared to a single-pass test. This extra time allows for static recrystallization to occur between passes. Furthermore, test T-2 was performed with the high-level strain rate and slower cooling rate, both thought to encourage static recrystallization.

Test T-3 achieved only 20% recrystallization, occurring exclusively on grain boundaries. The unrecrystallized grains were deformed, elongated in the longitudinal direction, and deformed annealing twins were present. No nuclei were present on the deformed annealing twins, indicating recrystallization occurs preferentially on grain boundaries. Test parameters indicate that the lack of recrystallization is due to low percent reduction, cooling during deformation, and a single pass.

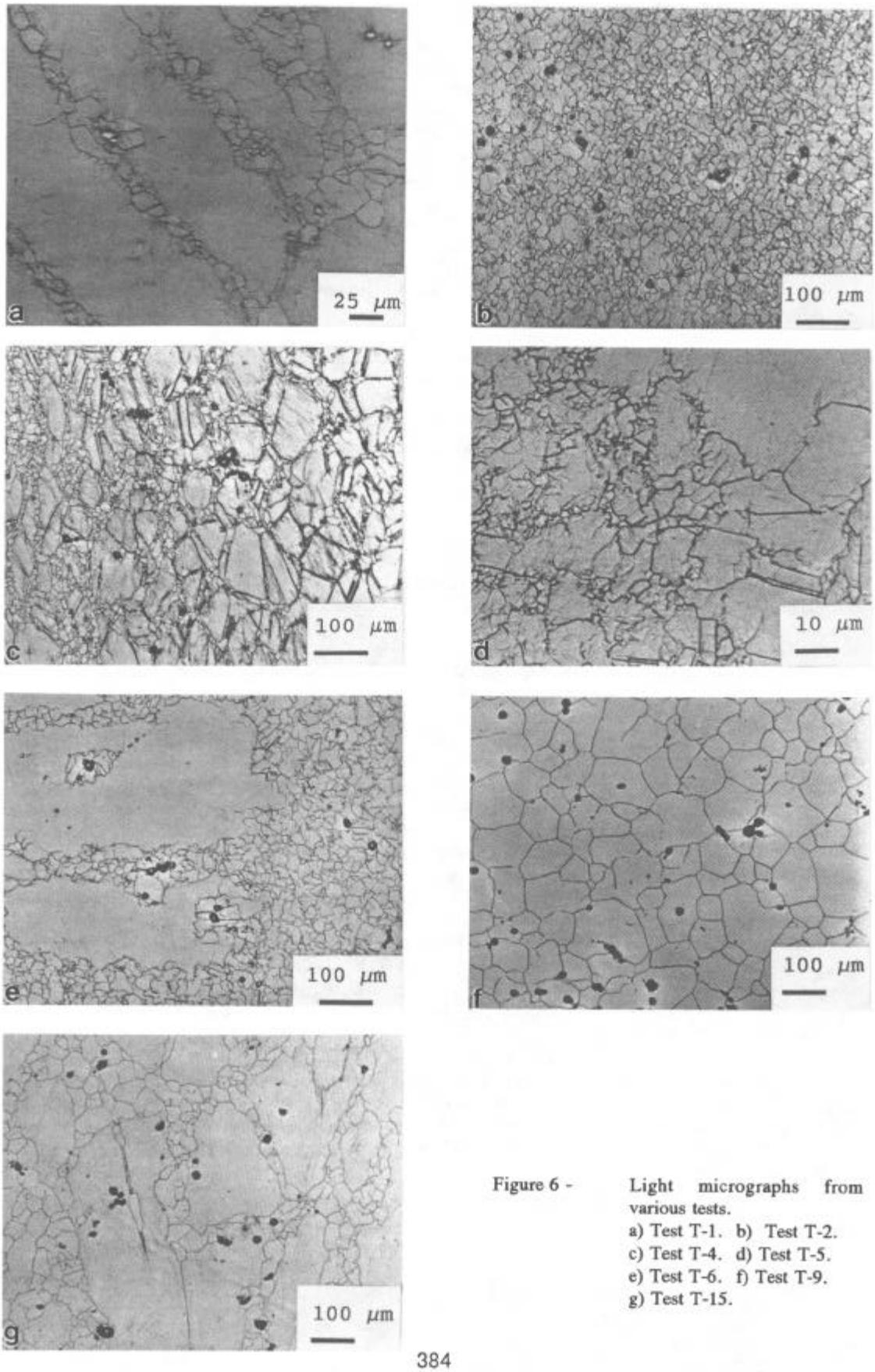

Figure 6 - Light micrographs from various tests.
a) Test T-1. b) Test T-2.
c) Test T-4. d) Test T-5.
e) Test T-6. f) Test T-9.
g) Test T-15.

A micrograph of test T-4 is shown in Figure 6c. Test T-4 achieved 65% recrystallization. Although tests T-4 and T-2 were both given similar reductions at the same temperature, the lower amount of recrystallization for test T-4 can be attributed to cooling during deformation. In addition to the loss of temperature following the final pass, which reduces recrystallization, at the lower forging temperature δ may precipitate upon cooling below 980 to 1000°C. This phase is known to reduce recrystallization by pinning high-angle boundary movement (16). In Figure 6c two distinct grain sizes are evident. It appears that the larger grain size (average 14 μm) recrystallized and coalesced during or after passes 1 and 2. The finer grains (average 3 μm) nucleated at grain boundary triple points after the following pass. This indicates that at least two separate recrystallization waves occurred, without the specimen achieving 100% recrystallization. Similar recrystallization behavior was observed by Mataya and Matlock (19) during multiple-stroke compression of alloy 718.

Test T-5 achieved 80% recrystallization. A high reduction percentage and lack of cooling during deformation caused the high recrystallization. An average grain size of 8 μm was measured. Figure 6d shows the increase in percent recrystallization from the edge to the center of test T-5. Nearly 100% recrystallization occurred at the center, and a necklace structure is evident closer to the edge. Only scattered nucleation occurred at the edge. This disparity is due to the nonuniformity of reduction throughout the specimen due to some barreling which was more pronounced in the highly deformed specimens. This edge-to-center effect was observed in all the low temperature tests to varying degrees, with the exception of test T-2.

Approximately 73% recrystallization was observed in test T-6, even though the strain was small (*i.e.*, 35% reduction. Factors that favored the high degree of recrystallization were no cooling during deformation and three passes. Two distinct grain sizes were apparent in some areas, once again indicating two separate waves of recrystallization. Figure 6e of specimen T-6 shows the fine recrystallization grains that have formed; however, a few large unrecrystallized grains still persist. Also observed was the nucleation of new grains occurring on some large carbides located within the unrecrystallized areas.

Test T-7 achieved 76% recrystallization and a fine recrystallized grain size of 8 μm. Extensive recrystallization resulted from the large percent reduction imparted to the specimen. The fine-grain size was due to the lower forging temperature, cooling during deformation, and the interaction of low forging temperature and cooling during deformation, which were the three most statistically significant influential factors/interactions in determining grain size according to the Taguchi analysis. Lower forging temperature and cooling during deformation leaves a lower temperature following deformation which inhibits grain growth. The interaction of forging temperature and cooling during deformation as the third most statistically critical source in determining grain size demonstrates that not only are the two factors critical but the effect is heightened when the high forging temperature is combined with cooling during deformation.

Test T-8 was a three-pass test with a combined reduction of 35% and cooling during deformation of 55.5°C. The test was similar to T-6 with respect to temperature, percent reduction, and number of passes, with the added feature of cooling during deformation. Test T-6, with about 73% recrystallization and a recrystallized grain size of 16 μm, can be compared to test T-8, which showed about 6% recrystallization and a recrystallized grain size of 6 μm. However, in test T-8 the grain size of the majority of the unrecrystallized matrix was estimated at 19 μm, which is much finer than the 72 μm starting grain size. This indicates, as in tests T-4 and T-6, that the matrix recrystallized substantially prior to the final pass. As opposed to test T-6, in which a high degree of recrystallization was achieved, the recrystallized matrix that is deformed in the final pass for test T-8 was unable to recrystallize, leaving fine deformed grains with minimal nucleation occurring at the grain boundaries. This was due to cooling during deformation and precipitation of the δ phase, both inhibiting recrystallization. Examination of the recrystallization of T-8 showed that many of the recrystallized grains had straight twin boundaries, substantiating that under certain conditions recrystallization may initiate due to twinning. It also indicates that the grains recrystallized statically.

Specimens Deformed at 1120°C

Hot deformation testing of tests T-9 to T-16 were performed at a temperature of 1120°C (2050°C), and all specimens, except test T-15, revealed a 100% recrystallized-grain structure. The structure coarsened to different degrees. No annealing twins were apparent in any of the specimens.

An example of the type of grain structure encountered with the high-temperature tests is given in Figure 6f. Notice that all the grains are nearly uniform in size with many of the grain boundaries forming triple points with nearly 120° angles, signifying that significant grain growth occurred. In single-phase alloys, grain growth slows dramatically or ceases when most of the triple point angles approach 120°, even though the grain size may be quite small. Tests T-11, T-12, and T-16 did not have as uniform or equiaxed structure as T-9, although they exhibited 100% recrystallization. Grain coarsening had not occurred to the same extent as the other tests. Furthermore, test T-15, which was cooled during deformation, Figure 6g, shows the same necklace, duplex grain size structure as observed in the lower temperature tests; however the entire structure (both large and small grains) is much coarser.

ANOVA Results for Percent Recrystallization

The results of the ANOVA for percent recrystallization as a response variable are listed in Table V. Table V shows the column in the orthogonal test matrix and factor (variable) associated with it, the corresponding variance, and percent contribution of that factor to percent recrystallization. The F ratio is also listed to show the confidence level of the factor affecting percent recrystallization.

As expected, deformation temperature, T_o, is the dominant variable in percent recrystallization, as recrystallization is a time-temperature dependent phenomenon. The F ratio indicates that with 99% confidence, temperature affects the percent recrystallization of the final microstructure. The percent contribution indicates the percent reduction in total variation that can be achieved if the given factor can be controlled precisely. Therefore, with precise control of forging temperature, variation in percent recrystallization in our simulated experiment can be reduced 37.5%.

Percent reduction follows as the second most statistically significant factor. A 90% confidence level was calculated for percent reduction affecting recrystallization percent. Increases in the percent reduction of a specimen will increase the amount of recrystallization observed due to an increase in intergranular defects, such as deformation bands and other strain-induced heterogeneities, that increase the stored energy in the grains and provide increased driving force for strain-relieving mechanisms. These defects may also act as sites for nucleation of new grains.

A 90% confidence level was not achieved by any of the remaining variables or interactions. This means that variance within a factor level cannot be statistically discerned from the variance between the two factor levels. However, this does not mean that the remaining factors had no actual effect on the outcome of recrystallization percent.

Cooling during deformation, ΔT_D, also was associated with a large variance, meaning that the overall difference between percent recrystallized with no ΔT_D and a ΔT_D of 55.5°C (100°F) was substantial, but could not be statistically verified. The effect of cooling during deformation was observed from inspection of the test specimens.

Of note are the factors that did not prove to be significant in the amount of recrystallization. Initial grain size, cooling rate after deformation, number of rolling passes, initial hold time, and strain rate all resulted in nearly negligible variance in the percent recrystallization response variable. The fact that initial grain size did not affect the amount of recrystallization for this study was verified by supplemental experiments which are described and discussed in another paper (20).

The final row in Table V, e_{pooled}, is a total of all the columns that do not represent main factors or the interactions. The variance is small, which leads to the belief that no major variables that may affect percent recrystallization in the simulation process were omitted.

The final column represents the minimum percent contribution associated with each variable. The calculation of the percent contribution for each variable subtracts the error variance for the test, and thus the total percent contribution does not total 100%.

Table V - Summary of ANOVA with Recrystallization Percent as Response Variable

Column	Variable	Sum of Squares	υ	Variance	F ratio	Percent Contribution
1	T_o	0.5867	1	0.5867	9.49*	37.5
11	r	0.3031	1	0.3031	3.69+	17.9
4	ΔT_D	0.1693	1	0.1693	1.85	8.7
13	$\dot{\epsilon}$	0.0795	1	0.0795	-	2.5
5	T_o x ΔT_D	0.0543	1	0.0543	-	-
8	N	0.0258	1	0.0258	-	-
3	T_o x t_o	0.0140	1	0.0140	-	-
2	t_o	0.0036	1	0.0036	-	-
7	$\dot{C}$	0.0027	1	0.0027	-	-
14	D_o	0.0013	1	0.0013	-	-
	e_{pooled}	0.21448	5	0.0429	-	14.8

* 99% confidence level
+ 90% confidence level

Table VI - Summary of ANOVA with Recrystallized Grain Size as Response Variable

Column	Variable	Sum of Squares	υ	Variance	F ratio	Percent Contribution
1	T_o	7564	1	7564	14.2*	49.5
4	ΔT_D	3585	1	3585	4.4+	23.0
5	T_o x ΔT_D	1663	1	1663	1.7	10.2
7	$\dot{C}$	624	1	624	-	-
14	D_o	411	1	411	-	-
8	N	240	1	240	-	-
11	r	148	1	148	-	-
3	T_o x t_o	88	1	88	-	-
2	t_o	5	1	5		
13	$\dot{\epsilon}$	4	1	4	-	-
	e_{pooled}	675	5	135	-	4.5

* 99% confidence level
+ 90% confidence level

ANOVA Results for Recrystallized Grain Size

Results for recrystallized grain size as a response variable are given in Table VI. Again temperature is the dominating factor. There is a 99% confidence level that it affects recrystallized-grain size and 49.5% contribution to variation in results. The data for recrystallized-grain size in Table IV show the obvious difference between the temperatures. The high-temperature tests have 100% recrystallization with significant grain growth. Whereas at low temperatures, primary recrystallization is still occurring. The energy provided by temperature is being used to complete the recrystallization.

Cooling during deformation is the second most influential factor with a 90% confidence level that it is significant. With temperature as the most important factor, it follows that a loss of 55.5°C will have a strong effect on grain growth at either forging temperature. Furthermore, at the lower forging temperature, the cooling may result in δ precipitation which would further inhibit grain growth (16).

The interaction of temperature and cooling during deformation was the third most critical factor. This implies that not only are the two factors important by themselves, but the combination of temperature and cooling during deformation is also of importance. The data show that the tests with cooling during deformation in both temperature ranges have finer-grain sizes in all cases except one. At higher temperatures the grain sizes are much coarser and the numerical differences in average grain size are much larger. For example, the difference in grain size between the largest and the second largest grain sizes at high temperature is 38 μm. This is much larger than the entire range of grain sizes in the low-temperature tests. Since the ANOVA uses an orthogonal statistical analysis, it appears that cooling during deformation makes a greater difference at high temperatures despite the low-temperature tests that are cooled through the delta solvus temperature. This clearly shows the dependence of grain coarsening on temperature.

Cooling rate follows as the next largest variance in results. Although statistically it cannot be said to be significant in the range of cooling rates employed in this experiment, it is logical to assume that cooling rate may have had a larger influence if a greater range had been used. The remaining variables were calculated to be statistically insignificant.

ANOVA Results for Hardness

The results for Rockwell hardness as a response variable are listed in Table VII. Cooling rate after deformation was by far the single most dominant factor. The slower cooling rate produced harder materials than the faster cooling rate, despite the slower cooling rate providing greater times at higher temperatures for increased recovery. This occurrence has also been observed by others in slow cool versus quenched condition of annealed product (21). One study (22) attributed the increase in hardness to the reprecipitation of grain boundary secondary carbides such as $M_{23}C_6$. However, as many metal carbides were observed in the specimens solutionized at 1100°C for one hour for the material that was investigated in the present study, it is unlikely that reprecipitation of carbides is the explanation for the observed hardening. The more likely conclusion is that the slower cooling rate allowed for significant nucleation of the hardening precipitates, γ' and γ'', upon cooling. Further evidence that the increased hardening is due to fine precipitates, with substantial hardening potential, is seen by comparing the individual tests T-3 and T-2. Although test T-2 was fully recrystallized and T-3 resulted in less than 20% recrystallization, T-2 with the slower cooling rate had a substantially higher hardness value.

Temperature caused the next largest variance in hardness, but a 90% confidence level was not realized. The fact that the cooling rate overshadowed the effects of forging temperature and percent reduction indicates that the precipitation hardening has a much larger influence on hardness than strain-relieving mechanisms, most notably amount of microstructural recrystallization.

The remainder of the factors of interest were statistically insignificant. The relatively small error indicates that all important factors were considered.

Table VII - Summary of ANOVA with Hardness as Response Variable

Column	Variable	Sum of Squares	υ	Variance	F ratio	Percent Contribution
7	$\dot{C}$	507.37	1	507.37	34.36*	69.8
1	T_o	110.25	1	110.25	2.56	14.2
4	ΔT_D	16.60	1	16.60	-	1.0
11	r	9.76	1	9.76	-	-
3	T_o x t_o	8.85	1	8.85	-	-
14	D_o	5.52	1	5.52	-	-
13	$\dot{\epsilon}$	4.41	1	4.41	-	-
2	t_o	3.61	1	3.61	-	-
5	T_o x ΔT_D	2.25	1	2.25	-	-
8	N	0.526	1	0.526	-	-
	e_{pooled}	44.91	5	8.98	-	6.3

* 99% confidence level
+ 90% confidence level

Table VIII - Summary of ANOVA with Load at 3.0 mm Stroke Displacement as Response Variable

Column	Variable	Sum of Squares (x 10^{-6})	υ	Variance (x 10^{-6})	F ratio	Percent Contribution
1	T_o	4.739	1	4.739	21.2*	64.2
13	$\dot{\epsilon}$	1.039	1	1.039	2.3	13.4
4	ΔT_D	0.526	1	0.526	-	6.4
5	T_o x ΔT_D	0.235	1	0.235	-	-
11	r	0.177	1	0.177	-	-
3	T_o x t_o	0.155	1	0.155	-	-
8	N	0.081	1	0.081	-	-
2	t_o	0.003	1	0.003	-	-
14	D_o	1.6×10^{-5}	1	1.6×10^{-5}	-	-
	e_{pooled}	0.347	6	0.062	-	5.1

* 99% confidence level
+ 90% confidence level

ANOVA Results for Load at 3.0 mm Displacement

The ANOVA for load at a 3.0 mm stroke displacement is shown in Table VIII. As expected, temperature was the dominant factor and the only factor above 90% confidence level in affecting the response variable. Strain rate was the variable causing the next largest variance. Statistically it did not have a 90% confidence level in affecting the load. However, it has been shown by Weis (23) that alloy 718 has a strain rate sensitivity of approximately 0.14 at 1010°C and 0.18 at 1120°C for a change in strain rate of 0.1 s^{-1} to 1.0 s^{-1}, similar to the strain rates used in this study. For the most part, the remaining variables were statistically insignificant, cooling during deformation ranking below strain rate. Obviously, percent reduction and cooling rate should have no discernable effect in the analysis. All the reductions are identical at this displacement of 3.0 mm. Cooling rate occurs after the displacement of 3.0 mm and should not influence the load value. It is interesting to observe that the initial grain size of the specimen is completely insignificant in a statistical sense, indicating the initial grain size no longer contributes to the flow stress at this juncture in the tests. This was investigated further and is reported elsewhere (20).

Summary

From the Taguchi experimentation it was found that the deformation temperature is the most statistically significant factor in affecting the percent recrystallization of ring-rolled alloy 718. It affects percent recrystallization with a 99% confidence level. The percent reduction is the second most statistically significant factor in affecting the percent recrystallization.

Temperature is the most statistically significant factor in effecting recrystallized grain size with a 99% confidence level. Cooling during deformation is the second most statistically influential factor with a 90% confidence level. The combination of these two factors show that recrystallized-grain size is strongly dependent on finishing temperature.

Cooling rate is the statistically dominant factor in effecting the hardness of the final microstructure. It was the only factor with a 90% or higher confidence level. Slower cooling rates produced significantly harder microstructures due to an increase in precipitation hardening.

Temperature is the most statistically significant factor in influencing the load at a 3.0 mm stroke displacement. It was the only factor with a 90% or higher confidence level.

Analysis of variance determined that the following factors could not be statistically verified as having an effect on the response variables: a) initial hold time, b) number of deformation passes, c) strain rate, and d) initial grain size within the range of those variables tested. However, this does not suggest that all those variables were completely insignificant, only that they could not be statistically verified.

Acknowledgements

The authors acknowledge the support of the Advanced Steel Processing and Products Research Center, an NSF Industry-University Cooperative Research Center at the Colorado School of Mines We also thank Standard Steel in Burnham, PA who supplied the alloy 718 material used in this study.

References

1. E.A. Loria, Preface from *Proceedings of the International Symposium on the Metallurgy and Applications of Superalloy 718*, ed. by E.A. Loria, TMS, Warrendale, PA, 1989, p v.

2. W.L. Kimmerle, M.T. Miglin, and J.L. Nelson, "Stress Corrosion Cracking of Alloy 718 in Pressurized-Water-Reactor Primary Water", in *Proceedings of the International Symposium on the Metallurgy and Applications of Superalloy 718*, ed. by E.A. Loria, TMS, Warrendale, PA, 1989, pp 417-426.

3. J.M. Oblak, D.F. Paulonis, and D.S. Duvall, "Coherency Strengthening in Ni Base Alloys Hardened by DO_{22} γ'' Precipitates", *Metallurgical Transactions*, Vol. 5, 1974, pp 143-153.

4. A.K. Jena, "On the Stability of Precipitate Phases in Nickel Base Superalloys" from *Material Science Forum*, Vol.3 , ed. by G.E. Murch, 1985 pp 281-290.

5. M. Sundararaman and P. Mukhopahyay, "Precipitation of the δ-Ni_3Nb Phase in Two Nickel Base Superalloys", *Metallurgical Transactions A*, Vol. 19A, 1988, pp 453-465.

6. G.E. Korth, "Effects of Various Parameters on the Fatigue Life of Alloy 718" in *Proceedings of the International Symposium on the Metallurgy and Applications of Superalloy 718*, ed. by E.A. Loria, TMS, Warrendale, PA, 1989, pp 457-476.

7. T. Banik, P.W. Keefe, G.E. Maurer and L. Petzold, "Ultra Fine Grain/ Ultra Low Carbon 718" in *Proceedings of the International Symposium on the Metallurgy and Applications of Superalloy 718, 625 and Various Derivatives*, ed. by E.A. Loria, TMS, Warrendale, PA, 1991, pp 913-924.

8. C.I. Garcia, D.E. Camus, E.A. Loria and A.J. DeArdo, "Microstructural Refinement of As-Cast Alloy 718 via Thermomechanical Processing" in *Proceedings of the International Symposium on the Metallurgy and Applications of Superalloy 718, 625 and Various Derivatives*, ed. by E.A. Loria, TMS, Warrendale, PA, 1991, pp 925-941.

9. N.A. Wilkinson, "Forging of 718 - The Importance of TMP", in *Proceedings of the International Symposium on the Metallurgy and Applications of Superalloy 718*, ed. by E.A. Loria, TMS, Warrendale, PA, 1989, pp 119-134.

10. P.J. Ross, *Taguchi Techniques for Quality Engineering*, McGraw Hill, New York, NY, 1988, pp 23-113.

11. D.A.K.C. Chang, "The Influence of Ingot Heterogeneity Upon the Hot Deformation of Alloy 718", M.S. Thesis, No. T3371, Colorado School of Mines, 1987.

12. A. Mitchell, "The Present Status of Melting Technology for Alloy 718" in *Proceedings of the International Symposium on the Metallurgy and Applications of Superalloy 718*, ed. by E.A. Loria, TMS, Warrendale, PA, 1989, pp 1-16.

13. K.O. Yu and J.A. Domingue, "Control of Solidification Structure in VAR and ESR Processed Alloy 718 Ingots" in *Proceedings of the International Symposium on the Metallurgy and Applications of Superalloy 718*, ed. by E.A. Loria, TMS, Warrendale, PA, 1989, pp 33-48.

14. J.M. Poole, K.R. Stultz and J.M. Manning, "The Effect of Ingot Homogenization Practice on the Structure of Properties of Wrought Alloy 718" in *Proceedings of the International Symposium on the Metallurgy and Applications of Superalloy 718*, ed. by E.A. Loria, TMS, Warrendale, PA, 1989, pp 219-228.

15. A.H. Jones, "An Overview of Alloy 718 in Large Structural Castings" in *Proceedings of the International Symposium on the Metallurgy and Applications of Superalloy 718*, ed. by E.A. Loria, TMS, Warrendale, PA, 1989, pp 307-318.

16. P.J. Diconza, R.R. Biederman and R.P. Sing, "Homogenization and Thermomechanical Processing of Cast Alloy 718" in *Proceedings of the International Symposium on the Metallurgy and Applications of Superalloy 718, 625 and Various Derivatives*, ed. by E.A. Loria, TMS, Warrendale, PA, 1991, pp 161-172.

17. S.S. Gorelik, *Recrystallization in Metals and Alloys*, Mir Publishers, Moscow, USSR, 1981, pp 38-44, 90-93, 193-203.

18. R.E. Reed-Hill, *Physical Metallurgy Principles*, Litton Educational, New York, NY, 1973, pp 267-296.

19. M.C. Mataya and D.K. Matlock, "Effects of Multiple Reductions on Grain Refinement During Hot Working of Alloy 718" in *Proceedings of the International Symposium on the Metallurgy and Applications of Superalloy 718*, ed. by E.A. Loria, TMS, Warrendale, PA, 1989, pp 155-167.

20. D.R. Nielsen, S.W. Thompson, C.J. Van Tyne and M.C. Mataya, "The Effect of Thermomechanical Processing on the Grain Size of Ring-Rolled Alloy 718", in preparation.

21. O.A. Onyewuenyi, "Alloy 718-Alloy Optimization for Applications in Oil and Gas Production" in *Proceedings of the International Symposium on the Metallurgy and Applications of Superalloy 718*, ed. by E.A. Loria, TMS, Warrendale, PA, 1989, pp 345-362.

22. W.C. Leslie, *The Physical Metallurgy of Steels*, McGraw Hill, New York, NY, 1981, p 43.

23. M.J. Weis, "The Hot Deformation of As-Cast Alloy 718", M.S. Thesis, No. T-3382, Colorado School of Mines, 1987.